



**HAL**  
open science

# Quantum Chemical Topology of the Electron Localization Function in the Field of Attosecond Electron Dynamics

Angela Parise, Aurelio Alvarez-Ibarra, Xiaojing Wu, Xiaodong Zhao, Julien Pilmé, Aurélien de la Lande

► **To cite this version:**

Angela Parise, Aurelio Alvarez-Ibarra, Xiaojing Wu, Xiaodong Zhao, Julien Pilmé, et al.. Quantum Chemical Topology of the Electron Localization Function in the Field of Attosecond Electron Dynamics. *Journal of Physical Chemistry Letters*, 2018, 9 (4), pp.844-850. 10.1021/acs.jpcllett.7b03379 . hal-03956855

**HAL Id: hal-03956855**

<https://hal.sorbonne-universite.fr/hal-03956855v1>

Submitted on 25 Jan 2023

**HAL** is a multi-disciplinary open access archive for the deposit and dissemination of scientific research documents, whether they are published or not. The documents may come from teaching and research institutions in France or abroad, or from public or private research centers.

L'archive ouverte pluridisciplinaire **HAL**, est destinée au dépôt et à la diffusion de documents scientifiques de niveau recherche, publiés ou non, émanant des établissements d'enseignement et de recherche français ou étrangers, des laboratoires publics ou privés.

# Quantum Chemical Topology of the Electron Localization Function in the Field of Attosecond Electron Dynamics

*Angela Parise<sup>†</sup>, Aurelio Alvarez-Ibarra<sup>†</sup>, Xiaojing Wu<sup>†</sup>, Xiaodong Zhao<sup>†</sup>, Julien Pilmé<sup>‡</sup>, Aurélien de la Lande<sup>†\*</sup>*

<sup>†</sup>: Laboratoire de Chimie Physique, Université Paris Sud, CNRS, Université Paris Saclay. 15  
avenue Jean Perrin, F91405 Orsay, France.

<sup>‡</sup>: Laboratoire de Chimie Théorique, Sorbonne Universités, Université Pierre et Marie Curie,  
CNRS, F75005 Paris, France.

## **Corresponding Author**

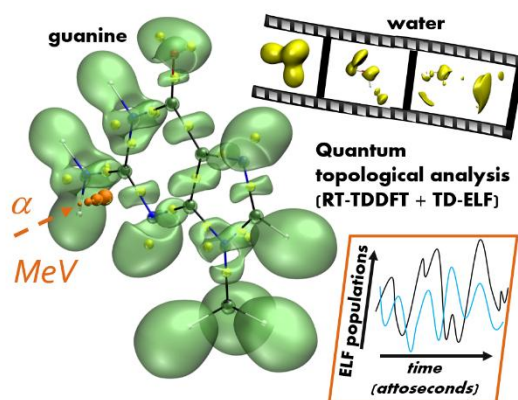
\*Aurélien de la Lande, [aurelien.de-la-lande@u-psud.fr](mailto:aurelien.de-la-lande@u-psud.fr)

## **ABSTRACT**

We report original analyses of attosecond electron dynamics of molecules subject to collisions by high energy charged particles based on Real-Time Time-Dependent-Density-Functional-Theory simulations coupled to Topological Analyses of the Electron Localization Function (TA-TD-ELF). We investigate irradiation of water and guanine. TA-TD-ELF enables qualitative and

quantitative characterizations of bond breaking and formation, of charge migration within topological basins, or of electron attachment to the colliding particle. Whereas the Lewis-VSEPR structure of gas phase water is blown out within a few attoseconds after collision, that of guanine is far more robust and reconstitutes rapidly after impact even though the molecule remains electronically excited. This difference is accounted by the presence of the electron bath surrounding the impact point which enables energy relaxation within the molecule. Our approach should stimulate future studies to unravel the early steps following irradiation of various types of systems (isolated molecules, biomolecules, nanoclusters, solids...) and is also readily applicable to irradiation by photons of various energies.

## TOC GRAPHICS



**KEYWORDS** quantum chemical topology, attosecond electron dynamics, radiation damages, DNA base, Real-Time TDDFT.

High energy charged particles (electrons, positrons, protons, alphas, hadrons...) interact with matter in turn inducing electronic excitations or ionization of the constituting molecules<sup>1</sup>. A fine understanding of irradiation is essential in various scientific domains. In astrochemistry ionizing radiations (IoR) deeply impact the complex chemistry occurring in gases or on grains<sup>2</sup>. In biology IoR cause deleterious damages to genomes, proteins or signaling pathways that normally regulate cell activity, having harmful consequences like accelerated aging, tumors and cancers<sup>3</sup>. Let us also mention that protection of astronauts from IoR is the major obstacle for planning human interplanetary travels. On the opposite, IoR have beneficial effects in proton- or hadron-therapies or for sterilization purposes in industry. Interaction of IoR with matter and their subsequent ultrafast consequences continues to challenge both experimental and computational approaches. Massive efforts push the development of attosecond sources, which in turn have started to stimulate new developments in computational physical chemistry<sup>4</sup>. In this Letter we are interested in deciphering the attosecond response of molecules' electron clouds submitted to ionizing radiations. We emphasize that collisions with charged particles are very different from absorptions of X-ray or UV/visible photons or from interactions of molecules with strong laser fields. Collision with keV-MeV alpha produces superposition of highly excited electronic states. The energy deposited locally into the electronic cloud is typically of several tens of eV. Although useful, the analysis of electron dynamics based on the occupations of molecular orbitals (MO) is cumbersome for these processes because of the very large number of involved MOs. The Electron Localization Function (ELF)<sup>5-6</sup> and its extension to the time domain<sup>7</sup> are alternative appealing tools. Two- or three dimensional plots of TD-ELF have been reported to describe alterations of molecular density fields when molecular systems interact with ultra-short laser pulses or collide with slow ions<sup>8-10</sup>. TD-ELF actually incorporates a valuable wealth of

information on the time evolution of the chemical structure that is potentially accessible by quantum topological analyses<sup>8, 11</sup>. We extend the analysis of ELF within the framework of gradient field theory which was initially developed for stationary electronic structures<sup>12-13</sup> to non-stationary electronic structures and apply it for the first time to irradiation of molecules by high energy alpha particles. Our approach enables, for instance, to qualitatively and quantitatively characterize formation/breaking of bonds between nuclei, electron flows (charge migration) among topological basins, or the attachment of electron density to the colliding particle. To illustrate the strength of the approach we successively consider collision of water or of a DNA base (guanine) by alpha particles and analyze the evolution of the ELF topological basins in combination with other descriptors of the electron dynamics.

Our electron dynamics simulations are based on Real Time TD-DFT<sup>14</sup> (Time-Dependent Density Functional Theory) which is a powerful theoretical approach to address attosecond dynamics of matter submitted to irradiation by laser field or charged particles<sup>15-23</sup>. We focus on inelastic collisions that are known to be largely dominant for kinetic energies of few tens of keV and higher<sup>1</sup>. The colliding particle is described as a point charge moving in space at constant velocity. The TD Coulomb potential created by the particle is included in the external Kohn-Sham potential. We use an implementation of RT-TDDFT in the deMon2k software<sup>24</sup> (see Reference <sup>25</sup> for details). All calculations have been done with the GGA (Generalized-Gradient-Approximation) CAP-PBE exchange-correlation potential<sup>26-27</sup>. CAP stands for Correct Asymptotic Potential and exhibits a correct  $1/r$  asymptotic behavior<sup>26</sup>. The capabilities of various XC functionals to fully capture the physics involved ionization by high energy particles are not yet fully understood. Global hybrids or range-separated hybrids would provide better

description of Rydberg or charge separated states than GGA which constitutes a limitation of the present protocol. More technical details on the simulation protocol can be found in SI.

The quantum chemical topology of ELF relies on the analysis of the gradient field of a scalar function by applying the theory of dynamical systems<sup>28</sup>. The latter provides a partitioning of the molecular space into non-overlapping volumes (basins). The ELF topology displays atomic and non-atomic maxima that can be related to chemical concepts issued from the Lewis theory. The core basins, labeled  $C(X)$  are located at nuclear centers, whereas the valence basins are located in the remaining space. These valence basins are characterized by a synaptic order, *i.e.* the number of core basins with which they share a common boundary<sup>13</sup>. Monosynaptic basins, labeled  $V(X)$ , usually associated to the lone-pair regions of  $X$  atoms, while disynaptic basins, labeled  $V(X, Y)$ , correspond to two-center covalent  $X$ - $Y$  bonds. Basins with a synaptic order of zero (termed as asynaptic) are sometimes found in the molecular space. They are labeled as  $V(A)$  in this work. The integration of the electron density over the basin volume provides a basin population or intrinsic moments<sup>29</sup>. Topological analyses have been performed with a modified version of the TOPCHEM package<sup>30</sup>.

Figure 1 depicts the total ionization cross section for water as a function of the kinetic energy of the colliding particle. Each point results from an average over one hundred trajectories with different initial positions of the alpha particle and impact parameter (see SI for details). RT-TDDFT results are in excellent agreement with the available experimental data<sup>31</sup>. Notably the maximum ionization probability around 0.1 MeV is recovered. RT-TDDFT results are also in good agreement with perturbative approaches such as the first Born Approximation Continuum Distorted Wave (FBA-CDW) or the Continuum Distorted Wave-Eikonal Initial State (CDW-EIS) methods<sup>32-33,31, 34</sup>. At higher energies the slope of the RT-TDDFT curve follows that of

standard models. The apparent capability of our RT-TDDFT implementation based on the CAP-PBE functional to simulate ionization by charged particles is in line with a few previous analogous simulations of collisions of water with fast protons<sup>16</sup>. These are encouraging results for future applications to large molecular systems.

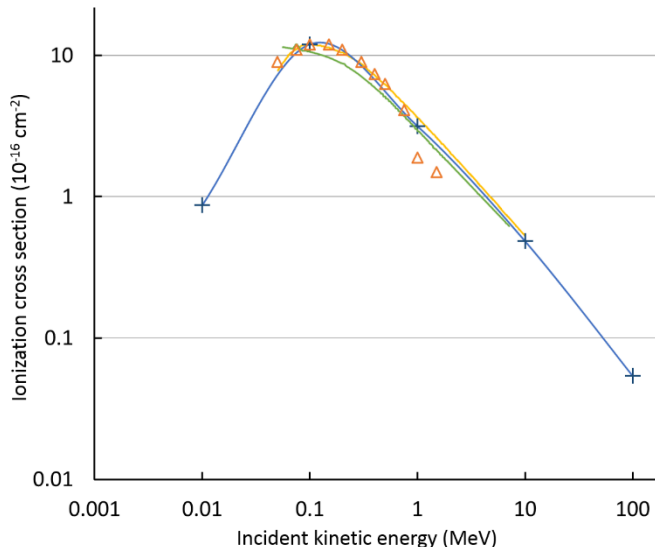


Figure 1: ionization cross-section for gas phase water. Ionization probability is calculated 1fs after collision. RT-TDDFT curve normalized to the experimental value for 0.1MeV. Blue line: RT-TDDFT; yellow: CDW-EIS model<sup>34</sup>; green: FBA-CDW model, orange triangles: experiments from Rudd et al<sup>31</sup>.

On the stationary electron density of isolated water obtained by a SCF (Self-Consistent-Field) procedure one recognizes on the ELF isosurfaces (Figure 2, Top) the well-known Lewis-VSEPR<sup>35</sup> structure comprised of oxygen core basin (C(O)), of two disynaptic protonated basins V(O,H) associated to O-H bonds and of two monosynaptic basins V(O) positioned around the HOH plane and associated to the oxygen lone pairs. The electron density integrated within the basins are also in line with the Lewis structure (e.g. around 2 electrons in the oxygen core shell, 2.3 in each lone pair...). We now consider five collisional trajectories with incident kinetic energies of 0.01, 0.05, 0.1, 1 and 100 MeV. We selected three snapshots for each trajectories (Figure 3); when the particle is approaching at 2 Å from H<sub>2</sub>O (Left), when it is within H<sub>2</sub>O

(Middle) and when it has moved 4 Å away from the molecule (Right). These distances refer to the van der Waals envelope of the molecule. Movies of ELF isosurfaces can also be found in SI for each of them.

The fastest particle (100 MeV) traverses the water structure causing only moderate perturbations to the ELF basins. After collision, periodic jiggling of the ELF basins are observed. They reflect Rabi oscillations among the excited electronic states populated by the transient collision. For impact energies of 1 MeV and below, we observe important modifications of the ELF already at the moment of collision. The formation of topological basins discloses probably the emission of electrons in Rydberg states or in the continuum. It is around 0.05-0.1 MeV that the perturbations seem to be the most severe, which corresponds to collision energies for which the amount of energy transferred to the molecule reaches a maximum (Figure S2). Note that the core basin C(O) remains undisturbed whatever the impact energy. On contrary to the stationary topology, the ELF valence regions seems to be scattered within the molecular space because many asynaptic valence basins (V(A)), not clearly associated to atoms, are observed (see Figure 3). These asynaptic basins appear as a typical signature of the intensity of collisions, although they are associated to small topological patches containing little electron densities.



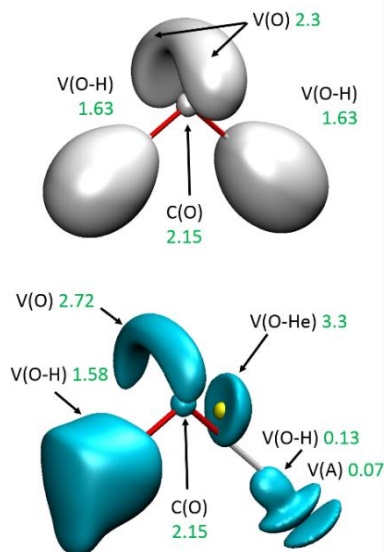


Figure 2: ELF isosurfaces (0.88) on the stationary electron densities of H<sub>2</sub>O isolated (Top) and in presence of He nucleus ( $\alpha$  particle, in yellow, Bottom). ELF topological basin populations are given in electron numbers.

Interestingly for energies of 1 and 100 MeV no ELF basins encompassing the helium nucleus are formed. We interpret this result as a consequence of the ultrashort timescale of the collision that doesn't enable the electron cloud to attach around the helium nucleus. On the opposite, for incident energies of 0.5 MeV and below, a disynaptic V(O, He) basin is formed when the He<sup>2+</sup> nucleus is present within the water electron cloud (pictures in the middle). This reflects transient formation of bond between these nuclei. For energies of 0.05 and 0.01 MeV the alpha particle leaves the molecule with a fraction of electron cloud. Large monosynaptic V(He) basins containing respectively 0.49 and 0.79 electrons are identified on Figure 3 for these energies. This feature is a clear signature of the so-called electron attachment channel that topological analyses of TD-ELF are able to capture. All the dynamical features outlined above are to be contrasted with the ELF topological analysis performed on a fictitious stationary electron density with the helium atom situated within the water molecule (Figure 2, bottom). A disynaptic basin V(O, He) is found which holds 3.3 electrons among which 0.48 are attributed to He. The comparison of

stationary (SCF) vs. propagated electron densities illustrates the existence of specific ELF topological patterns on the attosecond regime.

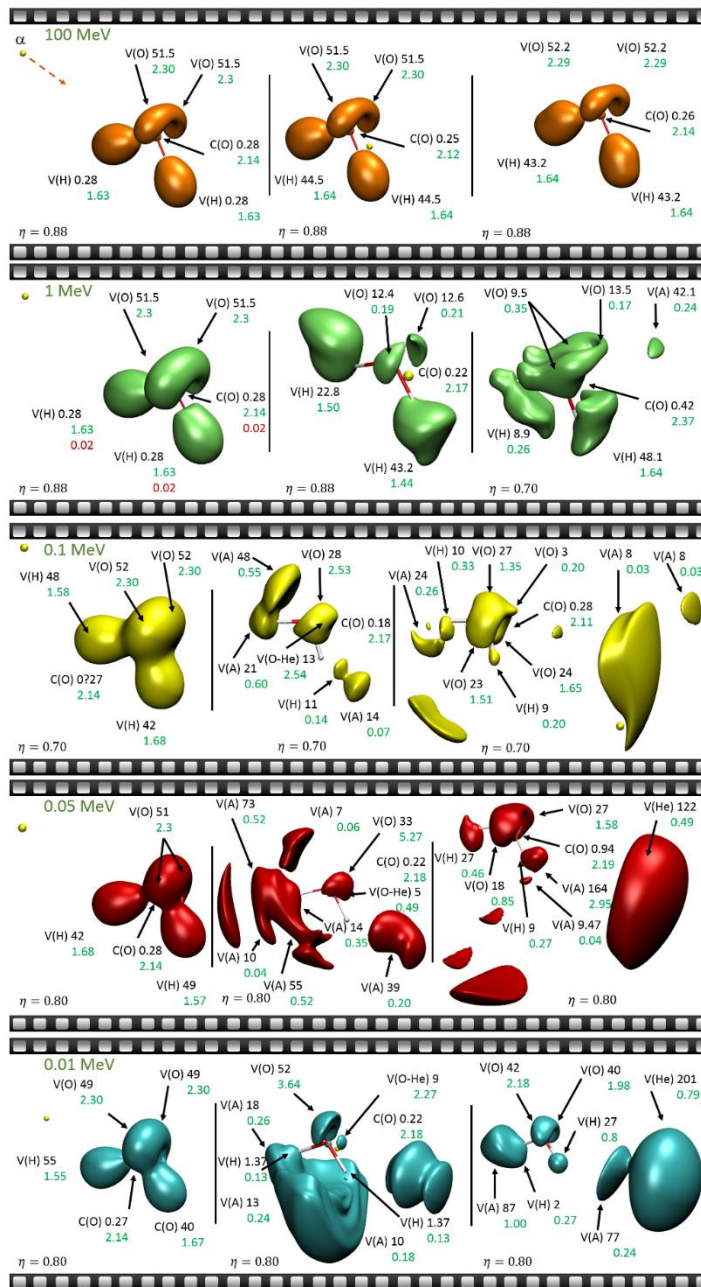


Figure 3: TD-ELF for water molecule impacted by alpha particles of various kinetic energies. For each topological basin we indicate, in order, the volume ( $\text{\AA}^3$ ) and the electronic population (in green). Some asymptotic basins are not labeled because they hold very little electron density and are thus not meaningful. Values of ELF isosurfaces are given for each picture.

As a second example, we report the collision of a guanine molecule impacted by an alpha particle travelling along a line perpendicular to the aromatic cycles. The kinetic energy of the particle is chosen to be 0.1 or 1MeV, the former being close to the maximum ionization probability as predicted by CDW-EIS models<sup>34</sup>. We also consider two impact points for guanine, either close to the central C=C bond (case *i*) or to the N-H group of the 6-member aromatic cycle (case *ii*). By convention the collision time corresponds to snapshot *a*. We focus first on case *i*) with a 1MeV particle and on the very moment of collision (snapshot *a-b*). We also encourage the reader to visualize the movies in SI. The ELF basins around the region of impact are drained by the +2 charge of the alpha particle. The V(C, C) basin is split into two monosynaptic V(C) basins, one located well above the aromatic plane in the direction of the helium atom, the other situated in opposite direction, *i.e.* below the plane. Together these two basins hold 3.5 electrons, which is close to the electronic population of the V(C, C) basins before collision (3.23, snapshot *a*). The intrinsic dipole moments within the monosynaptic V(C) basins are large, indicating strong polarization of the electron cloud caused by the collision. We also note the splitting of the unique V(C, O) basin associated on snapshot *a*) to the C=O bond into two basins comprising each, in average, 1.21 electrons. This is characteristic of a non-conjugated double C=O bond suggesting a weakening of electron delocalization among the aromatic cycle of guanine. As seen from a close examination of the central C-C region (see movies and Figure 4), the original bonding between central C-C atoms progressively reforms within a few hundreds of attoseconds after collision. The V(N) basins are also insightful. Those of nitrogens pertaining to the C=N-C groups belong to the  $\sigma$  system as reflected by ELF attractors lying within the aromatic plane. These basins are strongly affected by collision as seen from the large fluctuations of their electronic populations after disruption of the central C=C bond (Figure S11).

Furthermore these basins are occasionally split into sub-basins. The  $V(N)$  basins belonging to the  $\pi$  system (CNCCH<sub>3</sub> and CNHC) are situated above and below the aromatic plane. They are similarly impacted by collision since they transiently disappear and later reform. Altogether, these topological patterns indicate that both  $\sigma$  and  $\pi$  systems surrounding the impact point are contributing to the redistribution of the delivered energy through the entire molecule (around 67eV, Figure S3). To analyze more in depth the relaxation mechanism we computed the MO occupation numbers and the electronic kinetic energy integrated over atoms (Figures S4 and S9). Collision induces partial depopulation of all initially doubly occupied MOs, except those corresponding to core electrons. The latter point is corroborated by the ELF analysis on core basins (Figure S12). Meanwhile a wide manifold of initially unoccupied MOs acquire electronic populations, typically around 0.05  $e^-$ . We observe continuous fluctuations of occupation numbers in the rest of the simulation, indicating that the molecule remains in a highly excited state. Actually only a moderate fraction of the energy initially deposited by the collision is dissipated by ionization (Figure S3). The electronic kinetic energy integrated over atoms brings further insights into the relaxation mechanism. As expected, it is the atoms closest to the impact point that are the first ones to have their electronic kinetic energy increased, followed by fast (ca 100 as) energy damping and ultimately persistent oscillations on longer times. The other atoms respond with a delay depending on the distance from the impact point, the closer the atom to the impact the faster the local increase of electronic kinetic energy. The aforementioned features are signatures of intense dynamics taking place within the electron cloud even several hundreds of attoseconds after collision. This is also apparent in the movies showing the fluctuating TD-ELF isosurfaces. Somewhat surprisingly the Lewis structure of the molecule appears to be overall robust (see Figure 4 *f*). Simulations corresponding to case *ii*) (impact at the level of 6-members

ring NH group) with 1MeV particles lead to qualitatively similar conclusions. The main difference is that we observe initial disruption of the Lewis-VSEPR structure around the nitrogen atom, before relaxation. With 0.1 MeV alpha particles the energy delivered to the system is much higher (by a factor of almost two, Figure S3) and the electron cloud is clearly more affected. For instance the number of electron loss 2fs after collision, goes from ca 0.3 e- (1MeV) to 1.2 e- (0.1 MeV). Here again the ELF topological structure remains qualitatively robust (Figure S13).

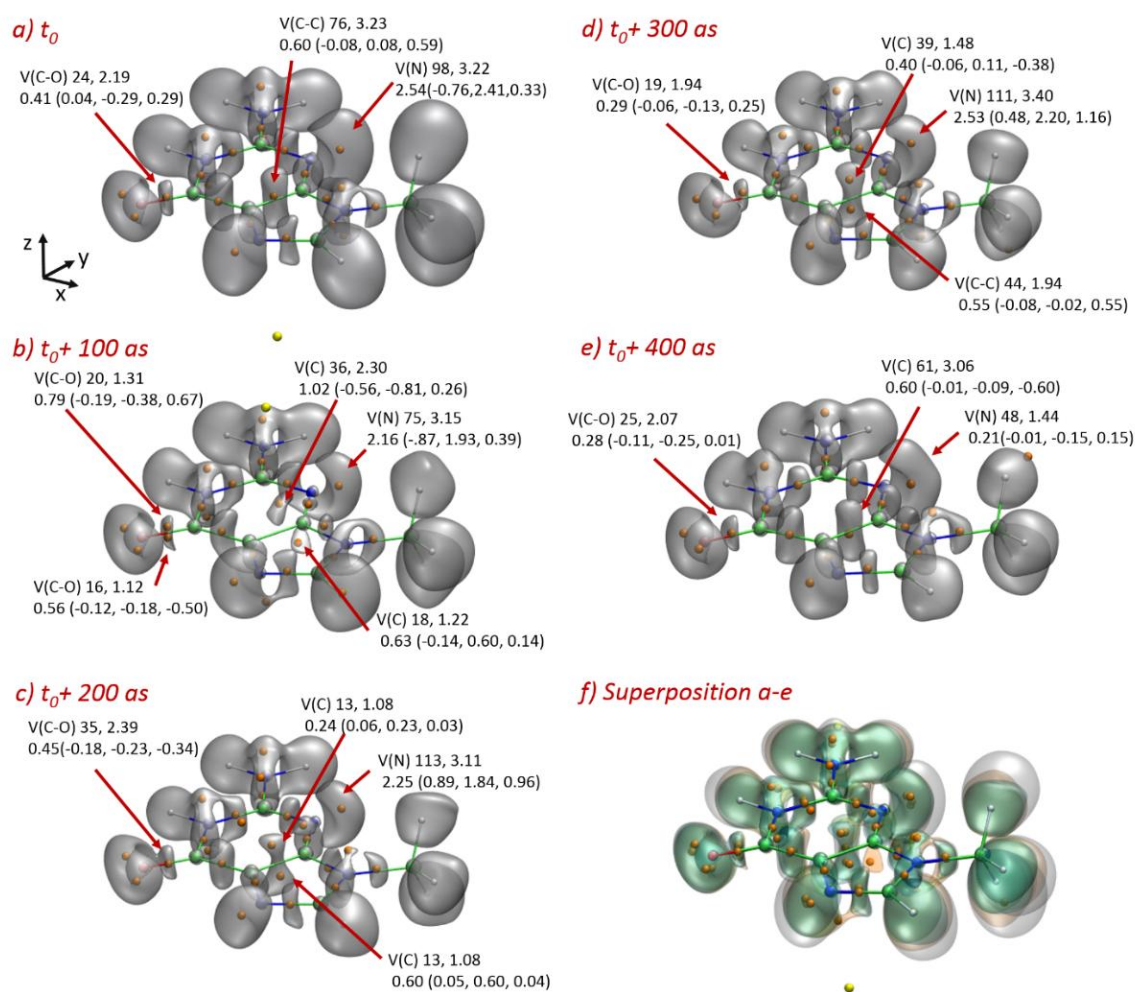


Figure 4: Topological analyses of TD-ELF after collision of guanine by a 1MeV  $\alpha$  particle travelling along the z direction. a-e: for each TD-ELF topological basins we indicate, in order, the volume ( $\text{\AA}^3$ ), the electronic population and the intrinsic dipole moment (D, components in brackets). f: superposition of ELF isosurfaces ( $\eta=0.8$ ) of snapshots a-d. Color code: green: carbons, white: hydrogens, blue: nitrogen, red: oxygen, yellow: helium ( $\alpha$  particle) and orange: off nuclei ELF attractors. See also SI for movies.

To conclude, the extension in this Letter of topological analyses of ELF in the context of collision of molecules by high energy charged particles has enabled a fine characterization of the induced attosecond electron dynamics. Other topological descriptors such as the delocalization index  $\delta_{AB}$ <sup>36</sup> could also be examined in the future. For irradiated guanine the ELF topology is surprisingly robust on the attosecond time scale despite the huge amount of energy deposited on the molecule upon collision. This overall stability of TD-ELF basins should however not mask the intense electron dynamics taking place within the electron cloud. Contrary to water, and presumably to other few atoms molecules, where ionization is the main relaxation pathway, guanine holds has a large enough electron cloud to relax energy, spreading out the deposited energy over the entire molecule. This may explain why the Lewis like structure is globally preserved even for 0.1MeV colliding particles. Nuclear motion should be included in future studies to account for energy dissipation into nuclear modes and possibly to fragmentations. Future studies will have to thoughtfully investigate the influence of environment on the very early steps following interaction of matter by IoR for example to characterize charge migrations or other ultrafast phenomena<sup>37</sup>. Recent implementations of RT-TDDFT within hybrid QM/MM schemes<sup>25, 38-39</sup> should find natural applications in that context. The herein presented analyzing tools should find a prominent place in such future investigations. We finally note that the herein developed approaches are readily application to other types of irradiations for example by photons.

## ASSOCIATED CONTENT

Computational details on RT-TDDFT simulations. Movies showing ELF isosurfaces for selected trajectories of water and guanine molecules (mpeg format). The following files are available free of charge.

## AUTHOR INFORMATION

The authors declare no competing financial interests.

## ACKNOWLEDGMENT

We thank Federica Agostini, David Lauvergnat and Mehran Mostafavi for several stimulating discussions and assistance in the preparation of the manuscript.

## REFERENCES

1. Mozumder, A., Interaction of Fast Charged Particles with Matter. In *Charged Particle and Photon Interactions with Matter*, CRC Press: 2003.
2. Dartnell, L. R., Ionizing Radiation and Life. *Astrobiol.* **2011**, *11* (6), 551-582.
3. Kryston, T. B.; Georgiev, A. B.; Pissis, P.; Georgakilas, A. G., Mutation Research/Fundamental and Molecular Mechanisms of Mutagenesis. *Role of oxidative stress and DNA damage in human carcinogenesis* **2011**, *711* (1-2), 193-201.
4. Lepine, F.; Ivanov, M. Y.; Vrakking, M. J. J., Attosecond molecular dynamics: fact or fiction? *Nat. Photon.* **2014**, *8* (3), 195-204.
5. Becke, A. D.; Edgecombe, K. E., A simple measure of electron localization in atomic and molecular systems. *J. Chem. Phys.* **1990**, *92* (9), 5397-5403.
6. Savin, A.; Jepsen, O.; Flad, J.; Andersen, O. K.; Preuss, H.; von Schnering, H. G., Electron Localization in Solid-State Structures of the Elements: the Diamond Structure. *Angew. Chem. Int. Ed.* **1992**, *31* (2), 187-188.
7. Burnus, T.; Marques, M. A. L.; Gross, E. K. U., Time-dependent electron localization function. *Phys. Rev. A* **2005**, *71* (1), 010501.
8. Castro, A.; Burnus, T.; L, M. M. A.; Gross, E. K. U., Time-dependent electron localisation function: A tool to visualise and analyse ultrafast processes. In *Analysis and Control of Ultrafast Photoinduced Reactions*, O. Kühn, L. W., Ed. Springer: Heidelberg, 2007; Vol. 87, pp 555-576.
9. Penka, E. F.; Couture-Bienvenue, E.; Bandrauk, A. D., Ionization and harmonic generation in CO and H<sub>2</sub>CO and their cations with ultrashort intense laser pulses with time-dependent density-functional theory. *Phys. Rev. A* **2014**, *89* (2), 023414.
10. Bruner, A.; Hernandez, S.; Mauger, F.; Abanador, P. M.; LaMaster, D. J.; Gaarde, M. B.; Schafer, K. J.; Lopata, K., Attosecond Charge Migration with TDDFT: Accurate Dynamics from a Well-Defined Initial State. *J. Phys. Chem. Lett.* **2017**, *8* (17), 3991-3996.
11. Pilmé, J.; Luppi, E.; Bergès, J.; Houée-Lévin, C.; de la Lande, A., Topological analyses of time-dependent electronic structures: application to electron-transfers in methionine enkephalin. *J. Mol. Model.* **2014**, *20* (8), 2368.
12. Piquemal, J. P.; Pilmé, J.; Parisel, O.; Gérard, H.; Fourré, I.; Bergès, J.; Gourlaouen, C.; de La Lande, A.; Van Severen, M. C.; Silvi, B., What can be learnt on biologically relevant systems from the topological analysis of the electron localization function? *Int. J. Quantum Chem* **2008**, *108* (11), 1951-1969.

13. Silvi, B.; Savin, A., Classification of chemical bonds based on topological analysis of electron localization functions. *Nature* **1994**, *371*, 683.
14. Runge, E.; Gross, E. K. U., Density-Functional Theory for Time-Dependent Systems. *Phys. Rev. Lett.* **1984**, *52* (12), 997-1000.
15. Zhang, C. L.; Hong, X. H.; Wang, F.; Wu, Y.; Wang, J. G., Theoretical investigation of He<sup>2+</sup>-Ar collisions in the energy range of 4-300 keV/amu. *Phys. Rev. A* **2013**, *87* (3), 032711.
16. Hong, X.; Wang, F.; Wu, Y.; Gou, B.; Wang, J., H<sup>+</sup>-H<sub>2</sub>O collisions studied by time-dependent density-functional theory combined with the molecular dynamics method. *Phys. Rev. A* **2016**, *93* (6), 062706.
17. Baxter, M.; Kirchner, T.; Engel, E., Time-dependent spin-density-functional-theory description of He<sup>+</sup>-He collisions. *Phys. Rev. A* **2017**, *96* (3), 032708.
18. Nagano, R.; Yabana, K.; Tazawa, T.; Abe, Y., Application of the time-dependent local density approximation to collision between a highly charged ion and an atom. *J. Phys. B: At., Mol. Opt. Phys.* **1999**, *32* (4), L65.
19. Dinh, P. M.; Reinhard, P. G.; Suraud, E., Dynamics of clusters and molecules in contact with an environment. *Phys. Rep.* **2010**, *485* (2-3), 43-107.
20. Wang, Z. P.; Dinh, P. M.; Reinhard, P. G.; Suraud, E.; Bruny, G.; Montano, C.; Feil, S.; Eden, S.; Abdoul-Carime, H.; Farizon, B.; Farizon, M.; Ouaskit, S.; Märk, T. D., Microscopic studies of atom-water collisions. *Int. J. Mass spectrom.* **2009**, *285* (3), 143-148.
21. Gao, C.-Z.; Wang, J.; Wang, F.; Zhang, F.-S., Theoretical study on collision dynamics of H<sup>+</sup> + CH<sub>4</sub> at low energies. *J. Chem. Phys.* **2014**, *140* (5), 054308.
22. Wang, J.; Gao, C.-Z.; Calvayrac, F.; Zhang, F.-S., Collision dynamics of proton with formaldehyde: Fragmentation and ionization. *J. Chem. Phys.* **2014**, *140* (12), 124306.
23. Covington, C.; Hartig, K.; Russakoff, A.; Kulpins, R.; Varga, K., Time-dependent density-functional-theory investigation of the collisions of protons and  $\alpha$  particles with uracil and adenine. *Phys. Rev. A* **2017**, *95* (5), 052701.
24. Köster, A. M.; Geudtner, G.; Alvarez-Ibarra, A.; Calaminici, P.; Casida, M. E.; Carmona-Espindola, J.; Dominguez, V.; Flores-Moreno, R.; Gamboa, G. U.; Goursot, A.; Heine, T.; Ipatov, A.; de la Lande, A.; Janetzko, F.; del Campo, J.-M.; Mejia-Rodriguez, D.; Reveles, J.; Vasquez-Perez, J.; Vela, A.; Zuniga-Gutierrez, B.; Salahub, D. R. *deMon2k Version 5*, Mexico City, 2016.
25. Wu, X.; Teuler, J.-M.; Cailliez, F.; Clavaguéra, C.; Salahub, D. R.; de la Lande, A., Simulating Electron Dynamics in Polarizable Environments. *J. Chem. Theor. Comput.* **2017**, *13* (9), 3985-4002.
26. Carmona-Espindola, J.; Gázquez, J. L.; Vela, A.; Trickey, S. B., Generalized gradient approximation exchange energy functional with correct asymptotic behavior of the corresponding potential. *J. Chem. Phys.* **2015**, *142* (5), 054105.
27. Perdew, J. P.; Burke, K.; Ernzerhof, M., Generalized Gradient Approximation Made Simple. *Phys. Rev. Lett.* **1996**, *77* (18), 3865-3868.
28. Silvi, B.; Gillespie, R. J.; Gatti, C., Electron Density Analysis A2 - Reedijk, Jan. In *Comprehensive Inorganic Chemistry II (Second Edition)*, Poeppelmeier, K., Ed. Elsevier: Amsterdam, 2013; pp 187-226.
29. Pilmé, J.; Piquemal, J.-P., Advancing beyond charge analysis using the electronic localization function: Chemically intuitive distribution of electrostatic moments. *J. Comput. Chem.* **2008**, *29* (9), 1440-1449.



30. Kozłowski, D.; Pilmé, J., New insights in quantum chemical topology studies using numerical grid-based analyses. *J. Comput. Chem.* **2011**, *32* (15), 3207-3217.
31. Rudd, M. E.; Goffe, T. V.; Itoh, A., Ionization cross sections for 10-300-keV/u and electron-capture cross sections for 5-50-keV/u  $^3\text{He}^{2+}$  ions in gases. *Phys. Rev. A* **1985**, *32* (4), 2128-2133.
32. Martinez, A. E.; Bullrich, J. A.; Maidagan, J. M.; Rivarola, R. D., The continuum distorted wave-eikonal initial state model for single electron capture in ion-atom collisions. *J. Phys. B: At., Mol. Opt. Phys.* **1992**, *25* (8), 1883.
33. Galassi, M. E.; Abufager, P. N.; Martinez, A. E.; Rivarola, R. D.; Fainstein, P. D., The continuum distorted wave eikonal initial state model for transfer ionization in  $\text{H}^+ + \text{He}^{2+} + \text{He}$  collisions. *J. Phys. B: At., Mol. Opt. Phys.* **2002**, *35* (7), 1727.
34. Quinto, M. A.; Monti, J. M.; Montenegro, P. D.; Fojón, O. A.; Champion, C.; Rivarola, R. D., Single ionization and capture cross sections from biological molecules by bare projectile impact. *Eur. Phys. J. D* **2017**, *71* (2), 35.
35. Gillespie, R. J., Fifty years of the VSEPR model. *Coord. Chem. Rev.* **2008**, *252* (12), 1315-1327.
36. Fradera, X.; Austen, M. A.; Bader, R. F. W., The Lewis Model and Beyond. *J. Phys. Chem. A* **1999**, *103* (2), 304-314.
37. Alexander, I. K.; Lorenz, S. C., Ultrafast correlation-driven electron dynamics. *J. Phys. B: At., Mol. Opt. Phys.* **2014**, *47* (12), 124002.
38. Morzan, U. N.; Ramírez, F. F.; Oviedo, M. B.; Sánchez, C. G.; Scherlis, D. A.; Lebrero, M. C. G., Electron dynamics in complex environments with real-time time dependent density functional theory in a QM-MM framework. *J. Chem. Phys.* **2014**, *140* (16), 164105.
39. Chen, H.; Ratner, M. A.; Schatz, G. C., QM/MM Study of Photoinduced Reduction of a Tetrahedral  $\text{Ag}_{20}^+$  Cluster by a Ag Atom. *J. Phys. Chem. C* **2014**, *118* (4), 1755-1762.